ACADEMIC PRESS

Available online at www.sciencedirect.com

SCIENCE DIRECT®

Journal of Solid State Chemistry 171 (2003) 308–312

JOURNAL OF SOLID STATE CHEMISTRY

http://elsevier.com/locate/jssc

Observation of the photon cascade emission process under $4f^15d^1$ and host excitation in several Pr^{3+}-doped materials

A.P. Vink,* P. Dorenbos, and C.W.E van Eijk

Interfaculty Reactor Institute, Delft University of Technology, Mekelweg 15, 2629 JB Delft, The Netherlands

Received 23 May 2002; received in revised form 10 July 2002; accepted 14 July 2002

Abstract

An overview is given of the research on the photon cascade emission (PCE) process for different Pr^{3+}-doped materials. The factors which determine the amount of emission originating from the second ($^3P_0/^1D_2 \rightarrow {}^{2S+1}L_J$) quantum cutting step are discussed and results on Pr^{3+}-doped hosts which show both the PCE process and parity-allowed $4f^15d^1 \rightarrow {}^{2S+1}L_J$ emission are reported. Lastly, the PCE process under host excitation with X-rays is discussed.

Keywords: Pr^{3+}; Photon cascade emission process; Host exatation

1. Introduction

The photon cascade emission (PCE) process is a process when one high-energy photon is absorbed resulting in a two-step emission process. In a theoretical paper, Dexter already predicted the existence of a photon cascade emission process (called: a "photon splitting" process) in 1957 [1], but the actual PCE process was discovered much later. This discovery was made in 1974 independently by two groups of scientists, whose discoveries on the luminescence of the lanthanide Pr^{3+} were both published in the same issue of the Journal of Luminescence [2,3].

The group of Sommerdijk from Philips Research Laboratories found the PCE process in the YF_3:Pr^{3+} and α-$NaYF_4$:Pr^{3+} materials when exciting with a Zn lamp [2], whereas Piper and co-workers from General Electric found the PCE process in a large number of Pr^{3+}-doped hosts, also including YF_3:Pr^{3+} and α-$NaYF_4$:Pr^{3+}, by excitation with a Hg lamp [3]. Piper already stated that, to obtain the photon cascade emission process, the $4f^2{}^1S_0$ level must be below the $4f^15d^1$ bands. Piper also measured Pr^{3+}-doped materials, like $LiYF_4$ where $4f^15d^14f^2$ emission was found [3].

For Pr^{3+}, the photon cascade emission process is visible by a number of emissions, basically in the spectral region from 215 nm all the way up to the infrared. The energy level scheme of Pr^{3+} is shown in Fig. 1. It shows excitation of the $4f^15d^1$ bands and a typical two-step emission, e.g., $^1S_0 \rightarrow {}^1I_6$ and $^3P_0 \rightarrow {}^3H_4$. The $^1S_0 \rightarrow {}^1I_6$ emission at about 400 nm always has the highest intensity. Pappalardo calculated the branching ratio for the different $^1S_0$ and other emissions in 1976 [4].

More than 20 years later new hosts were investigated, which also show the PCE process. Srivastava and co-workers found the photon cascade emission process in oxide hosts, like in $SrAl_{12}O_{19}$ [5], LaB_3O_6 [6] and $LaMgB_5O_{10}$ [7]. More recently the PCE process was also found in Pr^{3+}-doped $KMgF_3$ [8], $LiCaAlF_6$ and $LiSrAlF_6$ [9].

The photon cascade emission process became interesting for lighting applications, as in principle a quantum efficiency of 200% can be reached. Gaining extra quantum efficiency is interesting for using quantum cutting phosphors for a number of lighting applications, like flat television screen (PDPs). The excitation source in these applications is a xenon-discharge, of which emission is located below 200 nm and is peaking at 172 nm. The phosphors for television screens and lighting, which are used nowadays, cannot efficiently absorb this vacuum ultraviolet (VUV) radiation.

*Corresponding author. Fax: +31-1527-86422.
E-mail address: avink@iri.tudelft.nl (A.P. Vink).

0022-4596/03/$ - see front matter
doi:10.1016/S0022-4596(02)00183-4

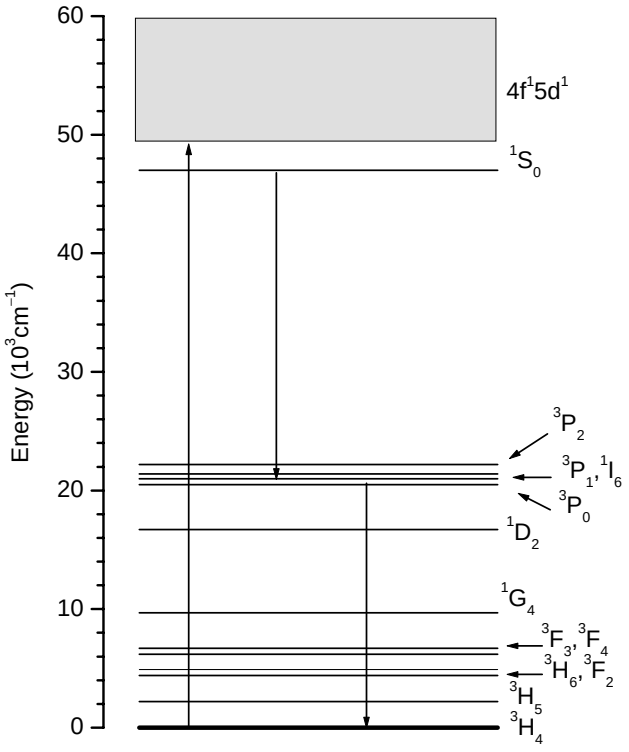

Fig. 1. Energy level scheme of Pr^{3+} showing a two-step emission ($^1S_0 \rightarrow {}^1I_6$ and $^3P_0 \rightarrow {}^3H_4$) after excitation in the $4f^15d^1$ bands. The non-radiative emission steps $4f^15d^1(1) \rightarrow {}^1S_0$ and $^1I_6 \rightarrow {}^3P_0$ are not shown.

The PCE process was not only found for Pr^{3+} ion, but also for other lanthanides. Wegh et al. found this effect, which was called quantum cutting for $LiGdF_4$:Eu^{3+} [10]. An advantage of using Eu^{3+} is that the two photons, emitted from the quantum cutting process, have the same energy. For Pr^{3+}, one photon is in the violet ($^1S_0 \rightarrow {}^1I_6$) and the other in the green ($^3P_0 \rightarrow {}^3H_4$) spectral region. A disadvantage of the Eu^{3+} quantum cutters is that the material has to be excited in a Gd^{3+} $4f^7$ line, which has a relatively small bandwidth and cross-section. The Pr^{3+} ion can be excited directly into the $4f^15d^1$ bands, which are broader and have a stronger absorption. Wegh also studied the quantum cutting system $LiGdF_4$:Er^{3+}, Tb^{3+} [11], but the quantum efficiency was lower than the $LiGdF_4$:Eu^{3+} phosphor.

We focussed on Pr^{3+}-doped quantum cutters. The PCE process was found for a number of different hosts like $LaZrF_7$ [12], α-$LaZr_3F_{15}$ [12], $BaSiF_6$ [13], $Sr_{0.7}La_{0.3}Al_{11.7}Mg_{0.3}O_{19}$ [14], SrB_4O_7 [14], $SrSO_4$ [15], $BaSO_4$ [15], $SrAlF_5$ [16] and $NaMgF_3$ [17].

In this paper general points for quantum cutting behaviour are discussed. At first, the second quantum cutting step is discussed, then the occurrence of both $4f^15d^1$ and $4f^2$ [$^1S_0$] emission in Pr^{3+} is reported. Lastly, the photon cascade emission process under X-ray excitation is reported.

2. Photon cascade emission process

2.1. Quantum efficiency of the second quantum cutting step

The most intense second quantum cutting step can either be $^3P_0 \rightarrow {}^3H_4$ or $^1D_2 \rightarrow {}^3H_4$ depending on the host. Generally, this is determined by the maximum phonon energy of the host. For quantum cutters with a small maximum phonon energy, the non-radiative relaxation from $^3P_0$ to $^1D_2$ is inefficient. An estimation of the transition probability can be made with the "van Dijk and Schuurmans" revised energy gap law [13]

$$W_{NR} = \beta_{el} \exp(-\alpha(\Delta E - 2\hbar\omega_{max})), \quad (1)$$

where W_{NR} is the non-radiative transition probability, $\beta_{el} = 10^7\,s^{-1}$, $\alpha = 4.5 \times 10^{-3}\,cm^{-1}$, ΔE is the energy difference between the $^3P_0$ and $^1D_2$ levels ($3700\,cm^{-1}$) and $\hbar\omega_{max}$ is the maximum phonon energy [13].

Inserting the typical phonon energy of a fluoride host of $500\,cm^{-1}$ [18] into Eq. (1) results in a non-radiative transition probability of about $53\,s^{-1}$, while inserting a phonon energy of $1410\,cm^{-1}$ for LaB_3O_6 [19] results in a value for W_{NR} of about $1.9 \times 10^5\,s^{-1}$. At this high phonon energy the non-radiative transition probability is large, whereas for the fluoride materials the non-radiative transition probability is much smaller than the radiative transition probability for the $^3P_0$ level of about $2 \times 10^4\,s^{-1}$ [13]. This explains why almost all oxide materials do not show any green $^3P_0$ emission. The only oxide material which shows green $^3P_0$ emission under $4f^15d^1$ excitation is $SrAl_{12}O_{19}$:Pr^{3+}. This behaviour can be explained by the low phonon energy (about $600\,cm^{-1}$) for this host.

For many oxide materials the intensity of the red $^1D_2 \rightarrow {}^3H_4$ emission is weak or even zero. A typical quenching process, called cross-relaxation, can explain the low intensity of the red emission. At high Pr^{3+} concentrations, cross-relaxation becomes more probable as two Pr^{3+} ions are involved. A visualisation of this process is shown in Fig. 2. In literature many different cross-relaxation processes are suggested, including $^1D_2 + {}^3H_4 \rightarrow {}^3F_4 + {}^3F_4$ [20–22]. Cross-relaxation decreases the radiative transition probability from the $^1D_2$ level. The quenching process from the $^3P_0$ level is less probable, as the energy mismatch (see Fig. 2) between the cross-relaxation steps, e.g., $^3P_0 + {}^3H_4 \rightarrow {}^1G_4 + {}^1G_4$, is large and the process therefore has to be strongly phonon-assisted.

2.2. The occurrence of both $4f^15d^1$ and $4f^2$ emission under vacuum ultraviolet excitation

In some Pr^{3+}-doped materials, both $4f^15d^1 \rightarrow {}^{2S+1}L_J$ and $4f^2[^1S_0 \rightarrow {}^{2S+1}L_J]$ was observed under excitation in the $4f^15d^1$ bands. In some materials, like CaF_2:Pr^{3+} [23]

the existence of two or more different cation sites can explain the emission behaviour. In the $BaSO_4:Pr^{3+}$ material only one Pr-site site is expected, but the two types of emissions were found. The intensity ratio between the $4f^15d^1 \rightarrow {}^{2S+1}L_J$ and $4f^2[{}^1S_0 \rightarrow {}^{2S+1}L_J]$ emissions also proved to be dependent on the temperature as is shown in the emission spectrum in Fig. 3. Also the decay time of the $^1S_0$ emission decreased with about a factor of three from 190 to 56 ns [24]. This typical behaviour was explained by thermal population of the $4f^15d^1$ band from the $^1S_0$ level. At higher temperature some of electrons will cross the energy barrier between the $^1S_0$ and the first $4f^15d^1$ band. By fitting the intensity ratio and the decay time a value for the energy barrier ΔE of about 0.04 ± 0.006 eV ($325 \pm 50\,cm^{-1}$) was found [24]. This value is about ten times smaller than the energy difference between the $^1S_0$ level and the first $4f^15d^1$ band $\Delta E_{^1S_0-4f5d}$ [24]. The smaller value for the energy barrier can be readily explained by the Stokes shift of about $4700\,cm^{-1}$ [25] thus lowering the intersection point of the two parabolas in the configurational co-ordinate model. Also the difference in shape of the parabola of the $4f^2$ and $4f^15d^1$ configurations can account for the differences in the value of the energy barrier and $\Delta E_{^1S_0-4f5d}$.

The process of thermal population is present for all Pr^{3+}-doped materials, which show the PCE process, but thermal population can only be observed at room temperature for materials where the $4f^15d^1$ bands are relatively close to the $^1S_0$ level.

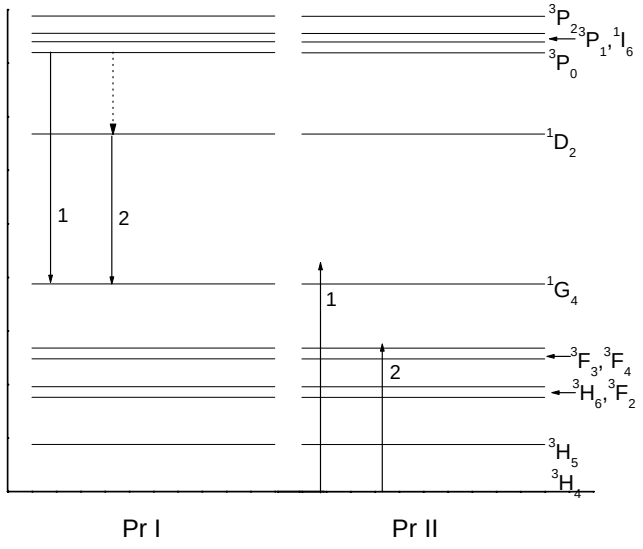

Fig. 2. The energy level scheme of Pr^{3+} up to $23{,}000\,cm^{-1}$. Possible cross-relaxation processes for the $^3P_0$ level (1) and the $^1D_2$ level (2) are shown. The non-radiative relaxation step from the $^3P_0$ to the $^1D_2$ level is shown as a dotted line. The non-radiative relaxation steps from the $^1G_4$(1) and the $^3F_4$ levels are not shown.

2.3. Quantum cutting under X-ray excitation

Quantum cutting can also be observed with Pr^{3+}-doped materials under excitation with X-rays. Srivastava et al. compared the emission properties of the $YF_3:Pr^{3+}$ material both under excitation with VUV radiation and with X-rays [26]. They reported no difference in the emission spectra under both types of excitation. Furthermore, they concluded that energy transfer from a localised electron–hole pair, self-trapped exciton (STE), to the Pr^{3+} can explain quantum cutting under X-ray excitation. More recently, a study of Pr^{3+}-doped materials was done under X-ray excitation in a number of materials, e.g., $SrAlF_5:Pr^{3+}$ [27]. Both studies were performed only at room temperature.

We performed a temperature dependent study ($T = 100-350$ K) of $SrAlF_5:Pr^{3+}$ under X-ray excitation.

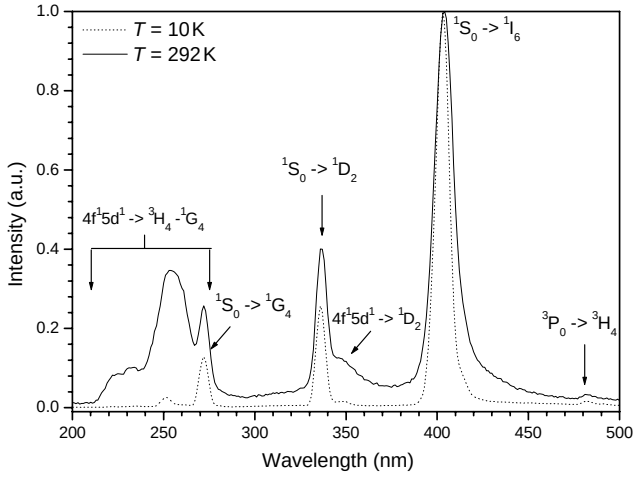

Fig. 3. Emission spectrum ($\lambda_{exc} = 188$ nm) of $BaSO_4:Pr^{3+}$ at $T = 10$ K (dashed line) and 292 K (solid line). The $4f^2$ and $4f^15d^1$ emission are assigned.

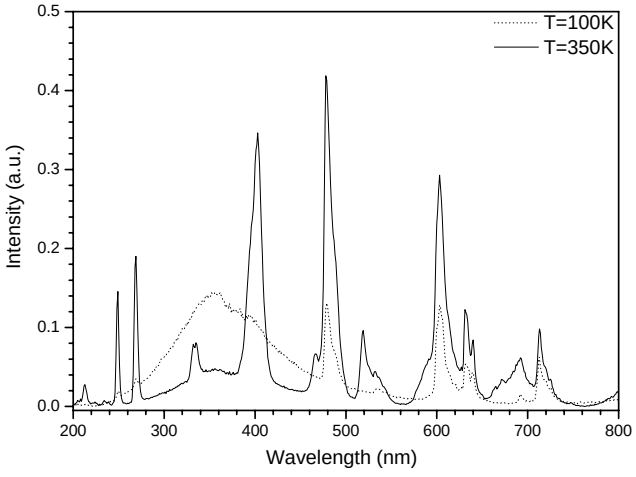

Fig. 4. X-ray excited emission spectra of $SrAlF_5:Pr^{3+}$ measured at $T = 100$ K (dotted line) and $T = 350$ K (solid line). The emission spectra are corrected for the response of the measuring system and photomultiplier.

In Fig. 4 the emission spectrum of $SrAlF_5:Pr^{3+}$ at $T = 100\,K$ and $T = 350\,K$ is shown. It can be observed that emissions from $^1S_0$ level are absent at 100 K temperatures, whereas they can be found at 350 K. Other emissions originating from the lower-lying Pr^{3+} levels, like $^3P_0$ and $^1D_2$ are however clearly visible at both temperatures.

At 100 K, broadband emission around 450 nm was found. This emission can be assigned to emission from a STE. At higher temperature energy transfer from the STE to the Pr^{3+} ion can occur. Energy transfer from the STE to the Pr^{3+} can explain the presence of Pr^{3+} emission from the lower-lying $^3P_0$ and $^1D_2$ levels, which is also present at $T = 100\,K$ (see Fig. 4).

It is however crucial for resonant energy-transfer to the $^1S_0$ level that the STE band extends up to the energy corresponding to the $^3H_4 \rightarrow {}^1S_0$ transition at a 215 nm. At 215 nm however no intensity from the STE can be found (see Fig. 4). Therefore, another process is responsible for the quantum cutting behaviour. This process is the direct recombination, without formation of a STE, of the electron and the hole with the Pr^{3+} ion. This process is well known for the Ce^{3+} ion and is responsible for the fast scintillation process. As the process of direct recombination is temperature independent, there must be explanation for the specific temperature behaviour, visible in Fig. 4.

A temperature dependent study of the intensity of the $^1S_0$ emission is presented in Ref. [16]. From this behaviour, it could be suggested that the hole is trapped on the Pr^{3+} ion forming Pr^{4+}, whereas the electron is trapped in a shallow electron trap. At higher temperatures these electrons are released from the trap and can recombine directly with the Pr^{4+} ion, resulting in Pr^{3+} in an excited state. From here the PCE process can occur, resulting in a two step emission to the ground state [16].

3. Conclusions

Three different features of the PCE process were discussed. The low-intensity of the second emission step in most oxide materials was explained by cross-relaxation, which has a high probability for the $^1D_2$ level. This level is populated by non-radiative relaxation from the $^3P_0$ to the $^1D_2$ state.

Furthermore, the occurrence of two different emissions for $BaSO_4:Pr^{3+}$ was explained by thermal population of the first $4f^15d^1$ band from the $4f^2$ $[^1S_0]$ level. An energy barrier was determined by both probing the intensity ratio between the two different emissions and the decay time of the $^1S_0$ level at different temperatures [24]. In principle this behaviour is present for all Pr^{3+}-doped quantum cutters, but can only be observed at room temperature for oxide hosts, where the energy difference between the first $4f^15d^1$ band and the $^1S_0$ level is relatively small.

Lastly, the PCE process under excitation with X-rays was discussed. It was found that two independent processes determine the typical behaviour at different temperatures. The first process is the formation of a STE, which can transfer its energy to the lower-lying $4f^2$ levels ($^3P_0$ and $^1D_2$) of the Pr^{3+} ion, whereas the $4f^15d^1$ bands are populated via direct recombination of the electron and hole on the Pr^{3+}. A temperature dependence of this direct recombination process suggests a rate-determining step, which is probably the release of an electron from a shallow trap.

Acknowledgments

The investigations, described in this paper were supported by the Dutch Technology Foundation (STW) and by the IHP-Contract HPRI-CT-1999-00040 of the European Commission.

References

[1] D.L. Dexter, Phys. Rev. 108 (1957) 630.
[2] J.L. Sommerdijk, A. Bril, A.W. de Jager, J. Lumin. 8 (1974) 341.
[3] W.W. Piper, J.A. deLuca, F.S. Ham, J. Lumin. 8 (1974) 344.
[4] R. Pappalardo, J. Lumin. 14 (1976) 159.
[5] A.M. Srivastava, W.W. Beers, J. Lumin. 71 (1997) 285.
[6] A.M. Srivastava, D.A. Doughty, J. Electrochem. Soc. 144 (1997) L190.
[7] A.M. Srivastava, D.A. Doughty, J. Electrochem. Soc. 143 (1996) 4113.
[8] I. Sokólska, S. Kück, Chem. Phys. 270 (2001) 355.
[9] S. Kück, I. Sokólska, J. Electrochem. Soc. 149 (2002) J27.
[10] R.T. Wegh, H. Donker, K.D. Oskam, A. Meijerink, Science 283 (1999) 663.
[11] R.T. Wegh, E.V.D. van Loef, A. Meijerink, J. Lumin. 90 (2000) 111.
[12] E. van der Kolk, P. Dorenbos, C.W.E. van Eijk, Opt. Commun. 197 (2001) 317.
[13] E. van der Kolk, P. Dorenbos, C.W.E. van Eijk, A.P. Vink, C. Fouassier, F. Guillen, J. Lumin. 97 (2002) 212.
[14] E. van der Kolk, P. Dorenbos, C.W.E. van Eijk, J. Phys.: Condens. Matter 13 (2001) 5471.
[15] E. van der Kolk, P. Dorenbos, A.P. Vink, R.C. Perego, C.W.E. van Eijk, A.R. Lakshmanan, Phys. Rev. B 64 (2001) 195129.
[16] A.P. Vink, P. Dorenbos, J.T.M. de Haas, H. Donker, P.A. Rodnyi, A.G. Avanesov, C.W.E. van Eijk, J. Phys. Condens. Matter 14 (2002) 8889.
[17] N.J.M. Le Masson, A.P. Vink, P. Dorenbos, A.J.J. Bos, J.P. Chaminade, C.W.E. van Eijk, J. Lumin. (2003), in press.
[18] A. Ellens, A. Meijerink, G. Blasse, J. Lumin. 59 (1994) 293.
[19] A. Ellens, B. Salemink, A. Meijerink, G. Blasse, J. Solid State Chem. 136 (1998) 206.
[20] H. Chen, R. Lian, M. Yin, L. Lou, W. Zhang, S. Xia, J.-C. Krupa, J. Phys.: Condens. Matter 13 (2001) 1151.
[21] H. Dornauf, J. Heber, J. Lumin. 22 (1980) 1.

[22] R.C. Naik, N.P. Karanjikar, M.A.N. Razvi, J. Lumin. 54 (1992) 139.
[23] K.D. Oskam, A.J. Houtepen, A. Meijerink, J. Lumin. 97 (2002) 107.
[24] A.P. Vink, P. Dorenbos, C.W.E. van Eijk, Phys. Rev. B 66 (2002) 75118.
[25] A.P. Vink, E. van der Kolk, P. Dorenbos, C.W.E. van Eijk, Opt. Commun. 210 (2002) 111.
[26] A.M. Srivastava, S.J. Duclos, Chem. Phys. Lett. 275 (1997) 453.
[27] P.A. Rodnyi, S.B. Mikhrin, P. Dorenbos, E. van der Kolk, C.W.E. van Eijk, A.P. Vink, A.G. Avanesov, Opt. Commun. 204 (2002) 237.